Dissertations, Master's Theses and Master's Reports

2016

Testing Lidar-Radar Derived Drop Sizes Against In Situ Measurements

Mary Amanda Shaw
Michigan Technological University, mashaw@mtu.edu

Recommended Citation

TESTING LIDAR-RADAR DERIVED DROP SIZES AGAINST IN SITU
MEASUREMENTS

By

Mary Amanda Shaw

A THESIS

Submitted in partial fulfillment of the requirements for the degree of

MASTER OF SCIENCE

In Applied Physics

MICHIGAN TECHNOLOGICAL UNIVERSITY

2016

This thesis has been approved in partial fulfillment of the requirements for the Degree of MASTER OF SCIENCE in Applied Physics

Department of Physics

Thesis Advisor: *Alexander G. Kostinski*

Committee Member: *Jacek Borysow*

Committee Member: *William I. Rose*

Department Chair: *Ravindra Pandey*

To my family, especially my eternal companion and most ardent supporter

"Whatever principle of intelligence we attain unto in this life, it will rise with us in the resurrection." (D&C 130:18)

Table of Contents

List of Figures

List of Tables

Acknowledgements

Thank you to my advisor Dr. Alexander Kostinski for his valuable feedback, direction, and ever present doubt.

Thank you to members of my committee for reading a dense, but short thesis.

Thank you to Dr. Edwin Eloranta of the University of Wisconsin-Madison for his helpful lidar and radar discussions.

Special thanks to Kamal Chandrakar and the π Chamber group for their efforts to obtain a laboratory cloud drop size distribution (DSD).

Thank you to my fellow graduate students who helped me to remember how to take a derivative after 20+ years away from school.

Thanks to my family, especially my eternal companion, for their support and sacrifice.

Finally, I thank Taco Bell for their family Taco Pack which helped to feed my family on many occasions so I could work on DSDs!

Abstract

How well can a co-located lidar and radar retrieve a drop size distribution in drizzling clouds? To answer, we mimic scattering from a laboratory cloud to retrieve a lidar-radar effective diameter $D'_{eff} = (\langle D^6 \rangle / \langle D^2 \rangle)^{1/4}$. Using only the shape parameter of the gamma-distributed drops, the mean diameter of the drops can be estimated from D'_{eff} to within a few percent of the true mean. In practice, the shape parameter of the gamma distribution is not known. To set bounds, mean diameters were calculated from D'_{eff} using a range of in situ measured gamma shape parameters. The estimated means varied within 13% below to 18% above the true mean. To put this range of inherent uncertainty for lidar-radar retrievals in perspective, a decrease of 15-20% in drop size is argued to be sufficient to offset a doubling of carbon dioxide concentrations (e.g., Slingo 1990).

1 Introduction

Clouds contribute a net cooling effect to the Earth's radiation budget (Ramanathan et al. 1989). Surprisingly, one cloud type in particular has the ability to influence Earth's radiation budget as much as increasing greenhouse gases do: stratocumuli (Wood 2012). Stratocumulus clouds cover more of the Earth than any other cloud type and small changes in their fractional coverage and thickness affect their albedo. Being able to accurately describe stratocumuli properties may lead to improved representation of stratocumulus clouds in global climate models, addressing a current challenge facing large scale models of the atmosphere (Kostinski 2008 and O'Connor et al. 2005).

In order to understand the macrophysical and microphysical processes in stratocumulus clouds, a detailed knowledge of the sizes of cloud and drizzle drops (a drop size distribution) is necessary. From a drop size distribution, cloud properties such as number density and mean diameter can be derived. Currently, drop size distributions are retrieved from: 1) in situ measurements made during field experiments and 2) measurements made by passive and/or active remote sensing systems. In situ measurements are considered more accurate, but suffer from the limitation that only small areas of the Earth can be covered at any given time (Miles et al. 2000). Considerable effort and emphasis has been focused on refining the retrieval methods associated with remote sensing due to the ability of remote sensing systems to monitor cloud properties on a continual basis while covering large areas of the globe.

Some remote sensing systems include a co-located cloud radar and high spectral resolution lidar (HSRL). The goal is to extract the drop size distribution parameters from the remotely sensed data, a not-so-easy task. As Bohren and Huffman (1983) illustrate it, remote sensing is similar to evaluating a dragon's footprints to obtain information about the size, shape, and height of the dragon. In our case, we will begin with the cloud drops sampled from a laboratory cloud (the dragon), create the lidar and radar footprints, and invert the process to determine how well we can reconstruct the original distribution.

Specifically, we test the ability to retrieve 1) the total number of drops in a sample volume and 2) the mean diameter of the gamma-distributed drops assuming the most ideal conditions: a single mode drop size distribution, perfectly aligned instruments, high signal to noise ratio, no multiple scattering, etc.

Donovan and van Lammeren (2001) suggest that cloud properties remotely sensed by a lidar-radar system can be described by the ratio of the sixth moment to the second moment of the distribution since radar backscatter is proportional to the sixth power of the drop diameter while the lidar extinction is proportional to the second power of the drop diameter. According to Mie theory, for a particle in the Rayleigh regime (i.e. the particle is much smaller than the wavelength as is the case of the radar and a drizzle or cloud drop) the scattering cross section of a particle is proportional to r^6/λ^4 where $r =$ radius and λ = wavelength. Inversely, for a particle in the geometric scattering regime (i.e. the particle is much larger than the wavelength as is the case of the lidar and a drizzle or cloud drop), the extinction cross section of a particle is proportional to its geometric cross section.

Stephens (1994) gives the equation for radar backscatter from a sample volume containing spherical drops:

$$\beta = \frac{\pi^5}{\lambda^4} k^2 \sum_{vol} D^6 = N \frac{\pi^5}{\lambda^4} k^2 \langle D^6 \rangle \qquad (1)$$

where β is the radar backscatter cross section, N is the total number of drops in the sample volume, λ is the wavelength of the radar (e.g. 3.2 mm), k^2 is the dielectric factor related to the index of refraction of water at the radar's wavelength, D is the diameter of the drops, and the brackets denote moment of the size distribution.

Although we know the number of drops and the diameters of the drops sampled from the laboratory cloud, this information would not normally be known to the remote sensor. Since there are two unknowns (the number of drops and the diameters of the drops), another measurement is needed. The HSRL extinction provides that second measurement. The lidar equation for the extinction cross section from a sample volume of

spherical drops is:

$$\alpha = \frac{\pi}{2} \sum_{vol} D^2 = N \frac{\pi}{2} \langle D^2 \rangle \tag{2}$$

where α is the lidar extinction cross section, N is the total number of drops in the sample volume, D is the diameter of the drops, and the brackets denote the moment of the size distribution (O'Connor et al. 2005). Combining equations 1 and 2 gives a value for D, a quantity based upon the ratio of the sixth moment to second moment. Therefore, we label it D'_{eff} the lidar-radar effective diameter:

$$D'_{eff} = \left(\frac{\lambda}{\pi}\right) \left(\frac{1}{2k^2}\right)^{1/4} \left(\frac{\beta}{\alpha}\right)^{1/4} . \tag{3}$$

In section 2, we discuss the gamma distribution as it applies to a cloud probability density function (PDF). In section 3, we fit a gamma distribution to the laboratory cloud PDF, calculate the lidar-radar effective diameter, and discuss how skewness and dispersion affect the normalized difference between the lidar-radar effective diameter and the mean diameter.

In section 4, we mimic scattering from the laboratory cloud to retrieve a lidar-radar mean diameter and total number of drops using the fitted gamma parameters of the laboratory PDF. We also test multiple gamma parameters derived from in situ measurements since in practice the gamma parameters are not known. Retrieval estimation error ranges are given.

In section 5, we create and randomly sample an ideal gamma distribution to test how the number of drops sampled by the lidar-radar system affects the retrieved quantities of the lidar-radar effective diameter and the lidar-radar mean diameter. Lastly, we test multiple gamma distribution parameters derived from many in situ measurements and give retrieval estimation error ranges for the total number of drops and the lidar-radar mean diameter.

2 The Gamma Distribution Applied to the Laboratory Cloud Probability Density Function (PDF)

The gamma distribution is commonly used to describe a cloud drop distribution (Stephens et al. 1990, Hu and Stamnes 1993, Miles et al. 2000, Donovan and van Lammeren 2001, O'Connor et al. 2005, Fielding et al. 2015). For this study, we have chosen to use a gamma probability density function that does not include the number density in order to minimize the number of free parameters:

$$f(D|a,b) = \frac{1}{b^a \Gamma(a)} D^{a-1} e^{-D/b} \tag{4}$$

where $f(D|a,b)$ has units of inverse length and is the probability density of finding a drop with a diameter between D and $D + dD$, D is the drop diameter with units of length, a is the unitless shape parameter, b represents the scale parameter with units of length, and $\Gamma(a) = (a-1)!$ represents the gamma function with argument a. The mean diameter (D_{mean}), mode diameter (D_{mode}), variance (σ^2), and coefficient of skewness (S) of the gamma distribution can be written as (Evans et al. 1993):

$$D_{mean} = ab \tag{5}$$

$$D_{mode} = b(a-1), a \geq 1 \tag{6}$$

$$\sigma^2 = ab^2 \tag{7}$$

$$S = 2a^{-1/2} \tag{8}$$

The moment (k) of the distribution is defined as (Petty and Huang 2011):

$$\langle D^k \rangle = \int_0^\infty D^k f(D|a,b) dD . \tag{9}$$

An effective (or equivalent) diameter, often used to quantify cloud optical properties, is the ratio of the third moment of the distribution to the second moment of the distribution (Stephens et al. 1990 and Hu and Stamnes 1993):

$$D_{eff} = \frac{\int_0^\infty f(D|a,b) D^3 \, dD}{\int_0^\infty f(D|a,b) D^2 \, dD} = \frac{\Gamma(3+a)b}{\Gamma(2+a)} = (a+2) \, b. \tag{10}$$

Note that Hu and Stamnes (1993), Stephens et al. (1990), and Miles et al. (2000) denote the scale parameter (b) as D_m and define it as a non-physical characteristic diameter (not

the mode diameter). In contrast, Donovan and van Lammeren (2001) set the scaling parameter (b) equal to the mode diameter (D_{mode}), thus defining the effective diameter in terms of the mode diameter. We argue that this is inappropriate because to do so would result in the following equation:

$$D_{mode} = (a - 1) \, D_{mode}. \tag{11}$$

The equality would only be true if the shape parameter (a) was equal to 2 and would force the mean diameter to always equal two times the mode diameter. These two restrictions would severely limit the parameters of the gamma distribution and would not describe the vast number of in situ measurements found in Miles et al. (2000) nor the laboratory cloud PDF. Without setting the scaling parameter equal the mode diameter, the effective diameter in terms of the mode diameter becomes:

$$D_{eff} = \frac{(a + 2)}{(a - 1)} \, D_{mode}. \tag{12}$$

The effective diameter in terms of the mean diameter is given by the equation:

$$D_{eff} = \frac{(a + 2)}{a} \, D_{mean}. \tag{13}$$

(As a side note, Hu and Stamnes (1993), Stephens et al. (1990), and Donovan and van Lammeren (2001) derive quantities in terms of radius rather than diameter.)

Returning to the definitions of D_{mean}, D_{mode}, and D_{eff} in terms of the two gamma parameters, we find that $D_{eff} \underset{limit}{\geq} D_{mean} \underset{limit}{\geq} D_{mode}$. Further, we derive how effective diameter deviates from the mean of the distribution in terms of only the shape parameter:

$$\frac{D_{eff} - D_{mean}}{D_{mean}} = \frac{2}{a}. \tag{14}$$

Since skewness is a function of only the shape parameter, $S = 2a^{-1/2}$, we can write skewness in terms of the normalized difference between the effective diameter and the mean diameter (i.e. an estimation error):

$$\frac{D_{eff} - D_{mean}}{D_{mean}} = \frac{S^2}{2} \tag{15}$$

which shows that as skewness increases, the difference between the effective diameter and the mean diameter increases and vice versa. Therefore, if a cloud PDF is highly skewed, we expect the effective diameter and mean diameter to differ and the amount they differ relates only to the shape parameter a.

For example, the software tool SBDART (Ricchiazzi et al. 1998) sets the shape parameter $a = 7$, giving the effective diameter (or radius) an estimation error of $\frac{D_{eff} - D_{mean}}{D_{mean}} = \frac{2}{a} = \frac{2}{7} * 100 = 30\%$. For the range of shape parameters given in Miles et al. (2000), $a = 8.6 +/- 7.3$, the estimation error ranges from 13% to 154%. Caution should be exercised when using the effective diameter rather than the mean diameter to compute physical properties. For example, the calculation of the liquid water content (LWC) based only upon the effective diameter can result in overestimating the LWC by more than a factor of two: $LWC = \left(\frac{D_{eff}}{D_{mean}}\right)^3 \approx (1.3)^3 \cong 2.2$.

As Donovan and van Lammeren (2001) suggest, cloud properties remotely sensed by a lidar-radar system are better described by the ratio of the sixth moment to the second moment of the distribution rather than the ratio of the third to second moment since radar backscatter is proportional to the sixth power of the drop diameter while the lidar extinction is proportional to the second power of the drop diameter. The ratio of the sixth to second moment yields a quantity defined as the lidar-radar effective diameter:

$$D'_{eff} = \left[\frac{\int_0^\infty f(D|a,b)\, D^6\, dD}{\int_0^\infty f(D|a,b)\, D^2\, dD}\right]^{1/4} = b\left[\frac{\Gamma(6+a)}{\Gamma(2+a)}\right]^{1/4} \qquad (16)$$

or in terms of the mean diameter and only the shape parameter (using equation 5):

$$D'_{eff} = \frac{1}{a}\left[\frac{\Gamma(6+a)}{\Gamma(2+a)}\right]^{1/4} D_{mean}. \qquad (17)$$

Again we compare how the lidar-radar effective diameter relates to the mean of the distribution in terms of only the shape parameter:

$$\frac{D'_{eff} - D_{mean}}{D_{mean}} = \frac{1}{a}\left[\frac{\Gamma(6+a)}{\Gamma(2+a)}\right]^{1/4} - 1. \qquad (18)$$

6

To determine the estimation error between the lidar-radar effective diameter and the mean diameter, we again use SBDART's shape parameter selection of $a = 7$:

$\frac{D'_{eff} - D_{mean}}{D_{mean}} = \frac{1}{a}\left[\frac{\Gamma(6+a)}{\Gamma(2+a)}\right]^{1/4} - 1 = \left(\frac{1}{7}\left[\frac{\Gamma(6+7)}{\Gamma(2+7)}\right]^{1/4} - 1\right) * 100 = 50\%$. Similar to the

effective diameter, caution should be exercised when using the lidar-radar effective diameter rather than the mean diameter to compute physical properties. For example, the calculation of the liquid water content (LWC) based only upon the lidar-radar effective diameter can result in overestimating the LWC by more than a factor of three: $LWC = \left(\frac{D_{eff}}{D_{mean}}\right)^3 \approx (1.5)^3 \cong 3.4$.

Skewness ($S = 2a^{-1/2}$) is only dependent upon the shape parameter (a) while variance ($\sigma^2 = ab^2$) and dispersion $\sigma = (ab)^{1/2}$ are dependent on both the shape parameter (a) and the scale parameter (b). However, for one PDF, the mean diameter ($D_{mean} = ab$) is a constant (C). Therefore, the variance (σ^2) and dispersion (σ) can be written in terms of only the scale parameter (b):

$$\sigma^2 = Cb \; ; \; \sigma = (Cb)^{1/2}. \tag{19}$$

In regional and global climate models the relative dispersion (also called the coefficient of variation) is a parameter commonly used to represent drop size distributions (Tas et al. 2015). Relative dispersion is of interest because our understanding of why drop sizes vary in a given environment is incomplete (Alexander Kostinski, personal communication, November 2015). The relative dispersion (ε), a ratio of the dispersion (σ) to the mean, can be defined in terms of only the gamma distribution shape parameter (a) or in terms of the skewness:

$$\varepsilon = a^{-1/2} \; or \; \varepsilon = S/2 . \tag{20}$$

Using SBDART's shape parameter selection of $a = 7$, we calculate a relative dispersion value of 0.38, a value slightly higher than the range of 0.25 to 0.35 given in Tas et al. (2015) for convective clouds. For the range of shape parameters given in Miles et al. (2000) for stratus clouds, $a = 8.6 +/-7.3$, the relative dispersion ranges from 0.25 to 0.88. The lower bound agrees with Tas et al. (2015), but the upper bound is much greater. Investigating the upper bound discrepancy is a topic for future research.

3 The Laboratory Cloud Probability Density Function (PDF)

Chang et al. (in review) have designed a cloud chamber capable of creating a steady-state cloud containing both cloud drops (diameters<50 microns) and drizzle drops (diameters≥50 microns). The resulting cloud PDF, with an applied gamma fit, is illustrated in Figure 3.1. Again, we have chosen to represent the distribution of drops as a
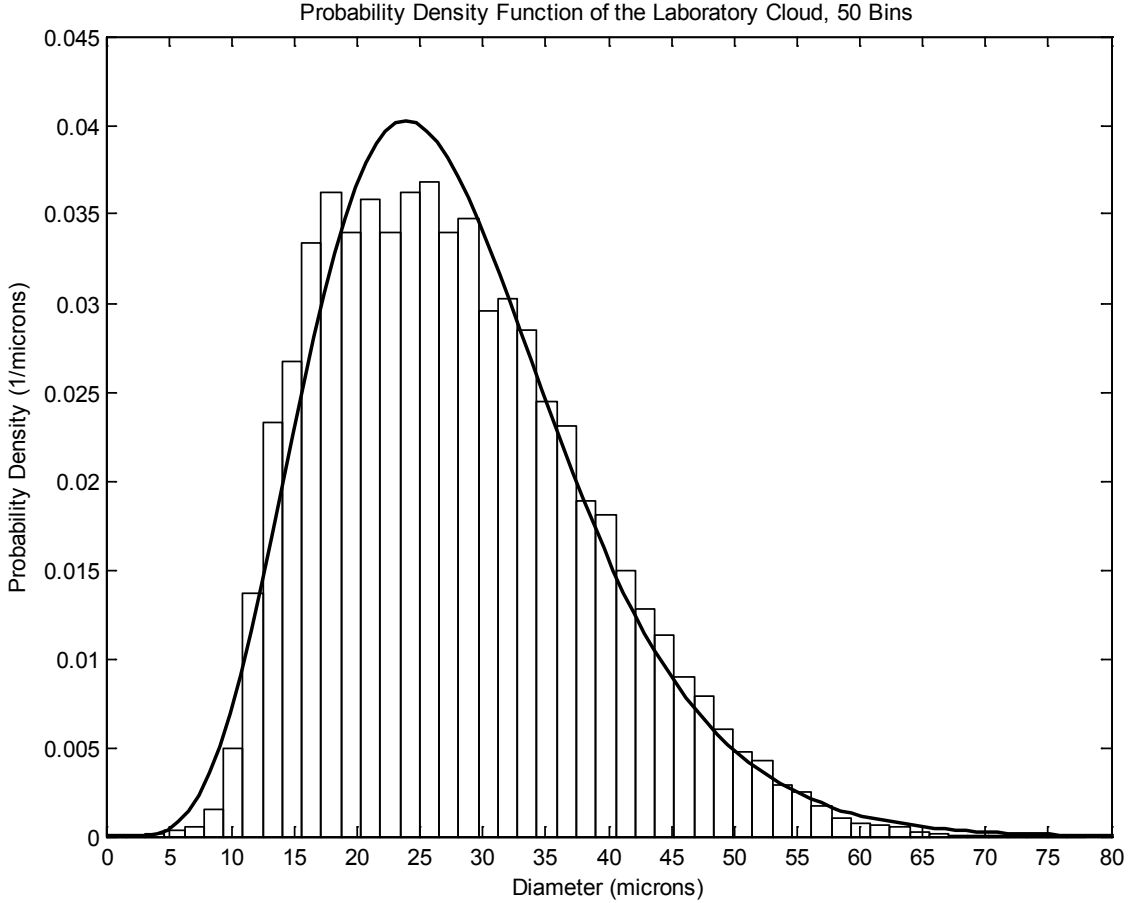

Figure 3.1: A laboratory cloud PDF is fitted with a gamma distribution in the form $f(D|a,b) = \frac{1}{b^a \Gamma(a)} D^{a-1} e^{-D/b}$ where a=7 and b=4 and bin width is 1.46 microns. The mean diameter is 27.9 microns, the skewness is $S = 2a^{-1/2} = 0.76$; the dispersion is $\sigma = a^{1/2}b = 10.6\ \mu m$ and the relative dispersion is $\varepsilon = a^{-1/2} = 0.38$. 87,000 drops were sampled from the steady-state cloud over a time period of approximately 10 hours, equaling a sample volume of ~355 cm³.

probability density function $\left(\int_0^\infty f(D|a,b)\,dD = 1\right)$ by not including the number density in order to reduce the number of free parameters.

Whether the laboratory cloud PDF is representative of one found in nature remains to be proven. However, the fitted gamma parameters fall within the mean and standard deviation of measured in situ gamma parameters compiled by Miles et al. (2000) for marine stratus cloud, but not for continental stratus clouds. Miles et al. (2000) gives the shape parameter mean and standard deviation of in situ measured (via airborne probes) marine stratus clouds as 8.6 +/- 7.3 and the scaling parameter mean and standard deviation as 2.7 +/- 2.0.

For the laboratory cloud PDF fitted with gamma parameters a=7 and b=4, the skewness is $2a^{-1/2} = 0.76$; the dispersion is $\sigma = a^{1/2}b = 10.6\ \mu m$; and the relative dispersion is $\varepsilon = a^{-1/2} = 0.38$. The relative dispersion of 0.38 is slightly higher than the range of 0.25 to 0.35 given in Tas et al. (2015) for convective clouds, but in the range of 0.25 to 0.88 calculated from the shape parameters given in Miles et al. (2000) for stratus clouds.

To determine how the gamma distribution parameters affect the skewness and the dispersion of the gamma distribution, we use the constant mean from the laboratory cloud PDF and vary the gamma parameters within the range given in Miles et al. (2000). Given equation 5 and a mean diameter of 27.9 microns, only certain gamma parameters are applicable. For example, using equation 5 with a shape parameter of 1.3 produces an associated scale parameter of 21 which does not fall within the in situ-measured scale parameter range of 0.7 - 4.7 given in Miles et al. (2000). Therefore, some shape and scale parameter combinations were discarded. The constrained shape parameter ranged from 6 to 15.9 and the constrained scale parameter ranged from 1.8 to 4.7.

Figure 3.2 illustrates that as the skewness increases, the estimation error of the lidar-radar diameter increases. Likewise, Figure 3.3 shows that the as the dispersion increases, the estimation error of the lidar-radar diameter increases.
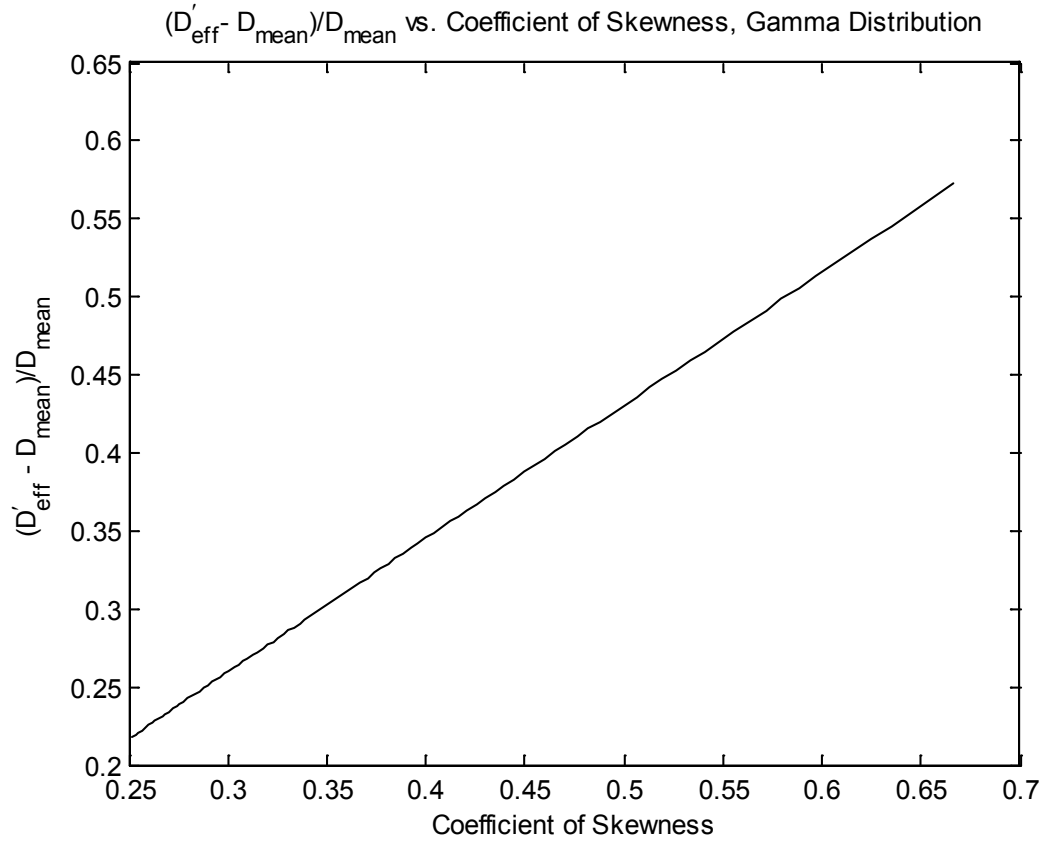
Figure 3.2: Varying the shape parameter (6 to 15.9) of the gamma distribution shows that as the coefficient of skewness ($S = 2a^{-1/2}$) increases, the normalized difference between the lidar-radar effective diameter and the mean increases.
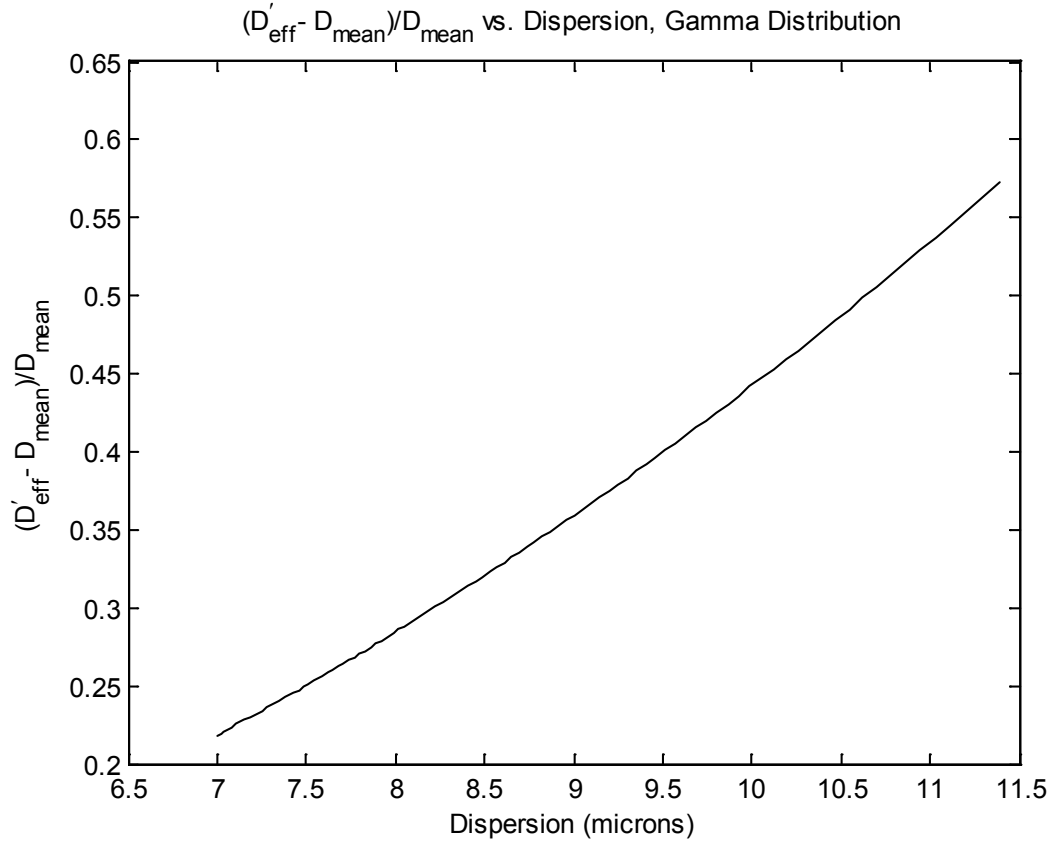
Figure 3.3: At a constant mean of 27.9 μm, as the dispersion ($\sigma = (Cb)^{1/2}$) increases, the normalized difference between the lidar-radar effective diameter and the mean increases. The scale parameter (b) varies between 1.8 and 4.7.

4 Simulated Scattering from the Laboratory Cloud Drops

First, we address the common assumption that the radar reflectivity in a drizzling cloud is dominated by the larger drizzle drops (O'Connor et al. 2005 and Fielding et al. 2015). We calculate the radar reflectivity and the lidar reflectivity of the laboratory drops as a function of the bin-center drop diameter, resulting values are illustrated in Figure 4.1. Here, we define reflectivity as the product of the number of drops in a histogram bin and either the sixth power (radar) or second power (lidar) of the bin-center drop diameter. Although the maximum number of drops occurs at the bin center diameter of 45 microns
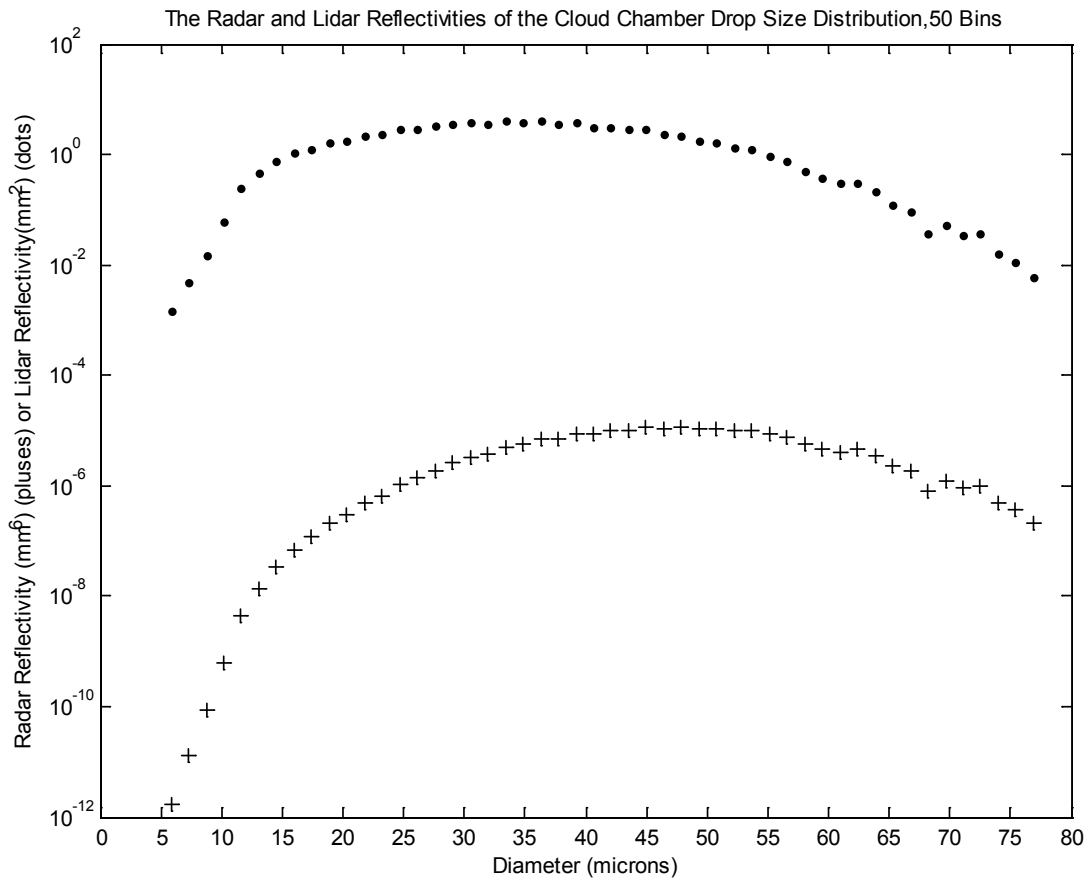
Figure 4.1: The radar reflectivity and the lidar reflectivity of the laboratory cloud is graphed as a function of bin-center drop diameter (bin width=1.46 microns). 91% of the drops are with the range of 15 microns to 65 microns and contribute 94% of the total radar reflectivity and 98% of the total lidar reflectivity. The maximum number of drops occurs at a bin center diameter of 45 microns for the radar and 33 microns for the lidar.

for the radar and 33 microns for the lidar, 91% of all drops fall within the range of 15 to 65 microns, contributing 94% of the total radar reflectivity and 98% of the total lidar reflectivity. Excluding the drops outside of the range of 15 to 65 microns results in an effective diameter of 39.9 microns which converts to a lidar-radar mean diameter (equation 22) of 26.8 microns, a 4% percent estimation error when compared to the true mean diameter of 27.9 microns. Therefore, at least for the laboratory PDF, the radar reflectivity is not dominated by the large drops simply because there are so few large drops. Hence the number of drops per diameter has a greater influence on the total reflectivity than the size of the drops.

For the 87,000 laboratory cloud drops, we calculate the lidar-radar effective diameter, the lidar-radar mean diameter, the total number of drops, and the estimation errors of each. Realizing that the gamma fit in shown in Figure 3.1 is not perfect, we expect the lidar-radar mean diameter and the total number of drops derived from the gamma moments and radar/lidar cross sections to differ from the true values. The lidar-radar effective diameter associated with the 87,000 drops is calculated using the equation (a form of equation 3):

$$D'_{eff} = \left[\frac{\sum_{vol} D^6}{\sum_{vol} D^2} \right]^{1/4}. \tag{21}$$

To calculate the lidar-radar mean diameter from the lidar-radar effective diameter, we rearrange equation 17:

$$D'_{mean} = a \, D'_{eff} \left[\frac{\Gamma(2+a)}{\Gamma(6+a)} \right]^{1/4} \tag{22}$$

where $a = 7$ is the shape parameter from the gamma fit shown in Figure 3.1. The total number of sampled drops (N) can be calculated from the lidar extinction cross section (equation 2) and the second moment of the distribution ($\langle D^2 \rangle$ from equation 9):

$$N = \frac{2}{\pi \langle D^2 \rangle} \alpha \tag{23}$$

or the radar backscatter cross section (equation 1) and the sixth moment of the

distribution ($\langle D^6 \rangle$ from equation 9):

$$N = \frac{\lambda^4}{\pi^5 k^2 \langle D^6 \rangle} \beta \qquad (24)$$

The estimations errors are computed using the following equations:

$$Estimation\ Error\ of\ D'_{eff} = \frac{D'_{eff} - D_{mean}}{D_{mean}} * 100 \qquad (25)$$

$$Estimation\ Error\ of\ D'_{mean} = \frac{D'_{mean} - D_{mean}}{D_{mean}} * 100 \qquad (26)$$

Note that D_{mean} and D'_{mean} are statistically different in that D'_{mean} is computed from D'_{eff} while D_{mean} (27.9 microns) is the true mean diameter of the 87,000 drops sampled from the laboratory cloud.

For the 87,000 laboratory drops, the lidar-radar effective diameter is 40.2 microns, yielding an estimation error of 44% from the mean (27.9 microns); the lidar-radar mean diameter computed from equation 22 is 26.9 microns, yielding a 4% estimation error; the total number of drops computed using equation 23 is 86,200 drops, yielding a few percent estimation error; and the total number of drops computed using equation 24 is 73,900 drops, yielding a 15% estimation error.

Assuming the shape and scale parameters were not known for the 87,000 drops, we set bounds using the gamma parameters given in Miles et al. (2000). The estimated means varied within 13% below to 18% above the true mean as shown in Figure 4.2. Figure 4.3 shows the estimation error associated with the total number of sampled drops (N) varied within 23% below to 27% above the true number of drops. Some shape and scale parameter combinations were discarded if outside the range given in Miles et al. (2000).
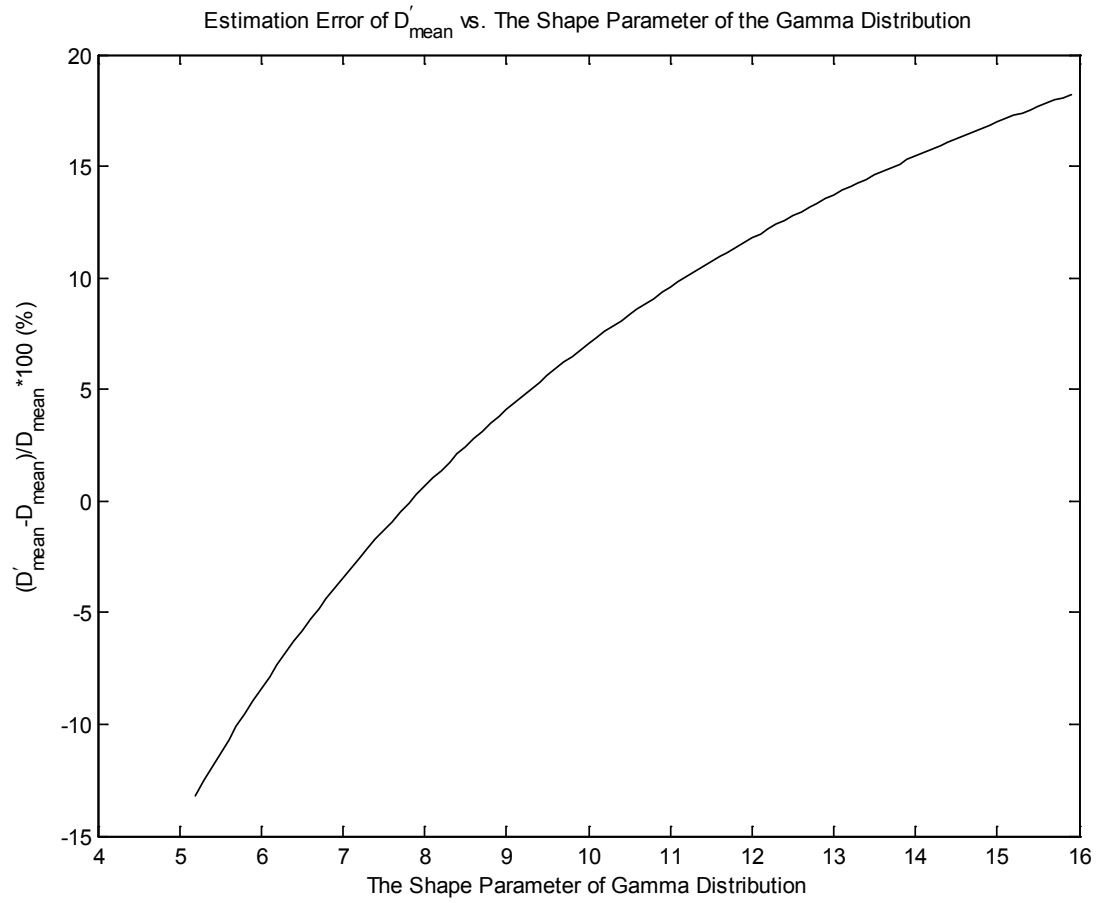
Figure 4.2: Using the lidar-radar effective diameter of the 87,000 laboratory drops and the shape parameter range of 5.2 to 15.9 from Miles et al. (2000), we show the estimation error of the lidar-radar mean diameter as a function of gamma distribution shape parameters.

The Estimation Error of the Retrieved Total Number of Drops vs.
The Shape Parameter of the Distribution

Figure 4.3: Using the simulated scattering from 87,000 laboratory drops and the shape parameter range of 5.2 to 15.9 from Miles et al. (2000), we show the estimation error of the total number of drops as a function of gamma distribution shape parameters. The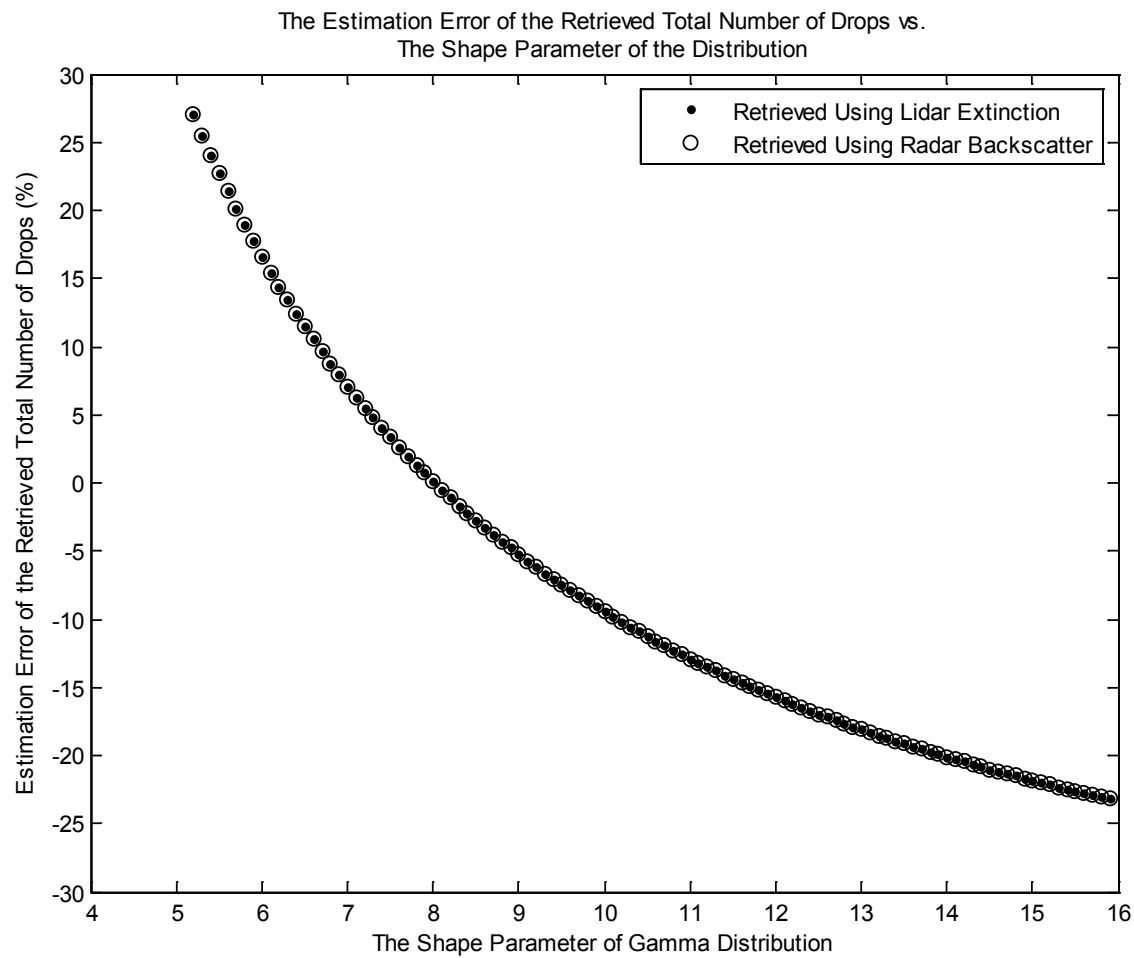 number of drops was computed using either the second moment of the distribution and the lidar extinction cross section (dots) or the sixth moment of the distribution and the radar backscatter cross section (circles).

5 Simulated Scattering from a Randomly Sampled Ideal Gamma Distribution

Due to the fact that lidars and radars sample a much larger number of drops than the number sampled from the cloud chamber, we have chosen to randomly sample the gamma distribution (shown in Figure 3.1) parameterized from the cloud chamber's 87,000 drops:

$$f(D|7,4) = \frac{1}{4^7\Gamma(7)} D^{7-1}e^{-D/4}. \tag{27}$$

This allows us to mimic the sampling of a much larger number of drops to see how the lidar-radar effective diameter (defined in equation 21) and lidar-radar mean diameter (defined in equation 22) vary with the sample size.

To sample, we create a cumulative distribution function (CDF), as shown in Figure 5.1, from the gamma distribution parameterized from the cloud chamber drops. Using numbers randomly drawn from a uniform distribution in the interval [0,1], we use the CDF to convert each random number to a drop diameter.

The number of drops sampled will depend upon the distance of the lidar and the radar to the sample volume. Sampling from spaceborne lidar-radar systems, because their footprints are very large due to their distance from the target, will image more drops than ground-based or aircraft-based systems. Of these three, aircraft-based systems due to their proximity to the sample volume will sample the smallest number of drops. However, even sampling with an in-cloud aircraft system will still allow for a large number of drops to be sampled compared to typical in situ or lab measurements.

For example, if the in-cloud lidar-radar system is imaging a sample volume between 62.5 and 100 meters above or below the lidar, the lidar will sample approximately 4 million drops. However, the aircraft radar, because of its larger beam width, will sample 3 billion drops at this same range, assuming 100 drops/cm^3 (see Appendix A). The results of sampling the distribution are presented in Table 5.1. Note that we chose to test very small, unrealistic lidar-radar samples to illustrate the dependence of sample size on the results.
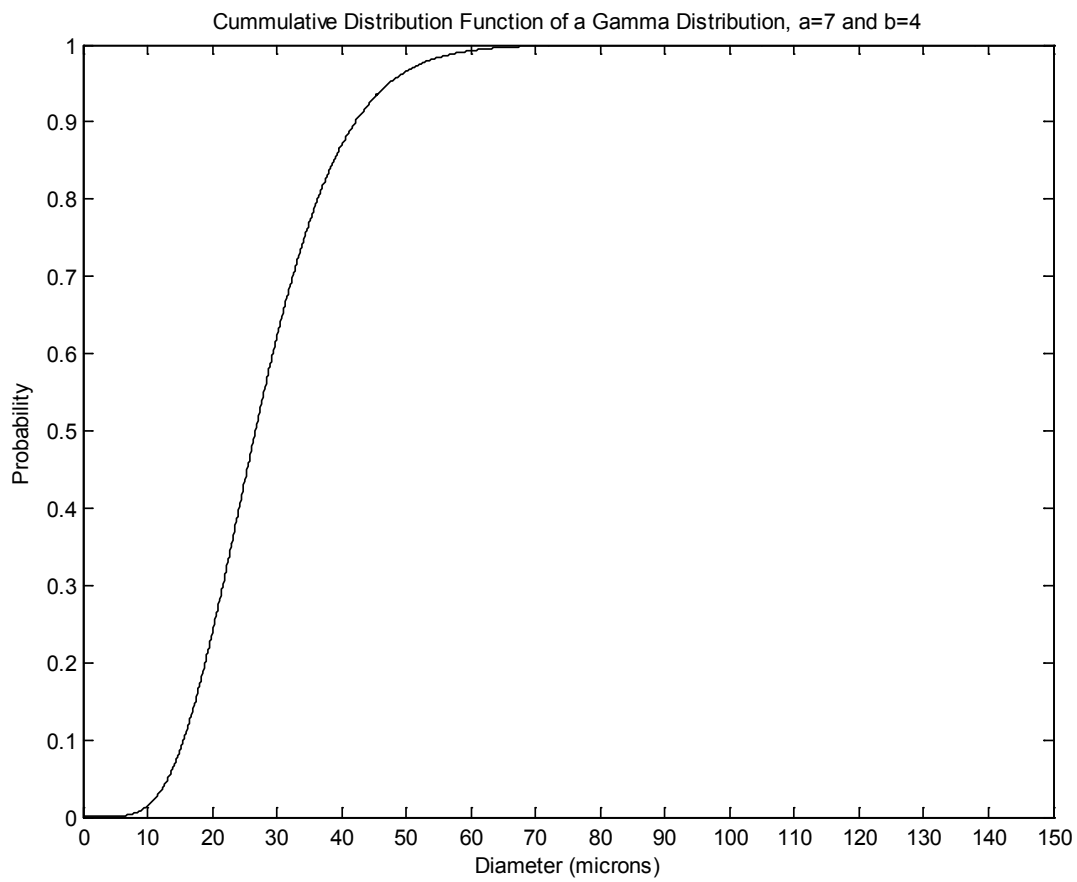
Figure 5.1: A cumulative distribution function is created from the gamma distribution of the cloud chamber drops.

Table 5.1: Lidar-Radar Simulated (Random) Sampling of the Gamma Distribution
Parameterized from the Cloud Chamber Drops

Sampling from an Ideal Gamma Distribution	Number of Drops Randomly Sampled	D'_{eff} (µm)	D'_{mean} (µm)	Estimation Error of D'_{eff}	Estimation Error of D'_{mean}
a = 7.0	1×10^3	44.8	30.0	60%	7%
b = 4.0	1×10^4	42.7	28.6	52.5%	2%
$D_{mean} = 28$ µm	1×10^5	41.9	28.1	49.6%	0.4%
	1×10^6	41.7	28.0	48.9%	0%
	1×10^7	41.8	28.0	49.3%	0%
	1×10^8	41.8	28.0	49.3%	0%

When the gamma distribution parameters are well known and sampled drops are greater than 10,000, the percentage change of D'_{mean} is insignificant. However, we have assumed that the lidar and radar illuminate the same number of drops which is not the case. Table 5.2 illustrates the results of varying the number of drops sampled by the radar versus the lidar. To be able to compute the lidar-radar effective diameter, an allowance is made for the difference in volume by multiplying the total lidar extinction cross section by a volume factor equal to the ratio of the radar volume to the lidar volume (Case 1 in Table 5.2).

Using the ratio of the sample volumes assumes that the cloud is homogeneous which may or may not be true. To determine if this is a reasonable assumption, we also compute the lidar-radar effective diameter by dividing the total lidar extinction by the number of drops sampled by the lidar and dividing the total radar backscatter by the number of drops sampled by the radar (Case 2 in Table 5.2). Comparing the values in Table 5.2 shows that there is no appreciable difference between the two cases. Therefore, accounting for the ratio of volumes is sufficient to account for the sampling differences between the lidar and radar footprints assuming a cloud is statistically homogeneous.

Table 5.2: Accounting for the difference in the number of drops sampled by the lidar versus the radar: In Case 1, the volumes are made comparable by multiplying the total lidar extinction by the ratio of the radar volume to the lidar volume. In Case 2, the volumes are made comparable by dividing the total lidar extinction by the number of lidar-sampled drops and the total radar backscatter by the number of radar-sampled drops. No appreciable difference exists between the two cases.

Case		Number of Drops Sampled	D'_{eff} (μm)	D'_{mean} (μm)	Estimation Error of D'_{eff}	Estimation Error of D'_{mean}
1	Lidar	4×10^6	41.9	28.1	50%	0.7%
	Radar	3×10^9				
2	Lidar	4×10^6	41.8	28.0	50%	0.4%
	Radar	3×10^9				

Rarely are the distribution parameters of a cloud PDF well known in advance. Instead only the lidar-radar effective diameter is known. Therefore, we select parameters derived from many in situ measurements of marine stratus clouds compiled by Miles et al. (2000). Using the lidar-radar effective diameter from Case 1 in Table 4.2 (41.9 microns), we test the range of shape parameters from 1.3 to 15.9 and scale parameters from 0.7 to 4.7.

Note that because of equation 5, not all shape parameters and scale parameters in Miles et al. (2000) are appropriate for a lidar-radar effective diameter of 41.9 microns. For example, converting the lidar-radar effective diameter to the lidar-radar mean diameter (equation 22) using a shape parameter of 1.3 produces an associated scale parameter (equation 5) of 9 which does not fall within in situ-measured parameter range of 0.7 - 4.7 given in Miles et al. (2000). Therefore, some shape and scale parameter combinations were discarded. The constrained range for the shape parameter is 5.5 to 15.9 and the constrained range for the scale parameter is 2.2 to 4.7.

Figure 5.2 shows that the estimation error of the lidar-radar mean diameter varied within 8% below to 24% above the true mean. In addition to retrieving the mean diameter from the lidar-radar effective diameter, we retrieved the total number of drops in the sample volume using equations 23 and 24. Figure 5.3 shows that the estimation error associated with the total number of sampled drops (N) varied within 12% above to 30% below the true number of drops.
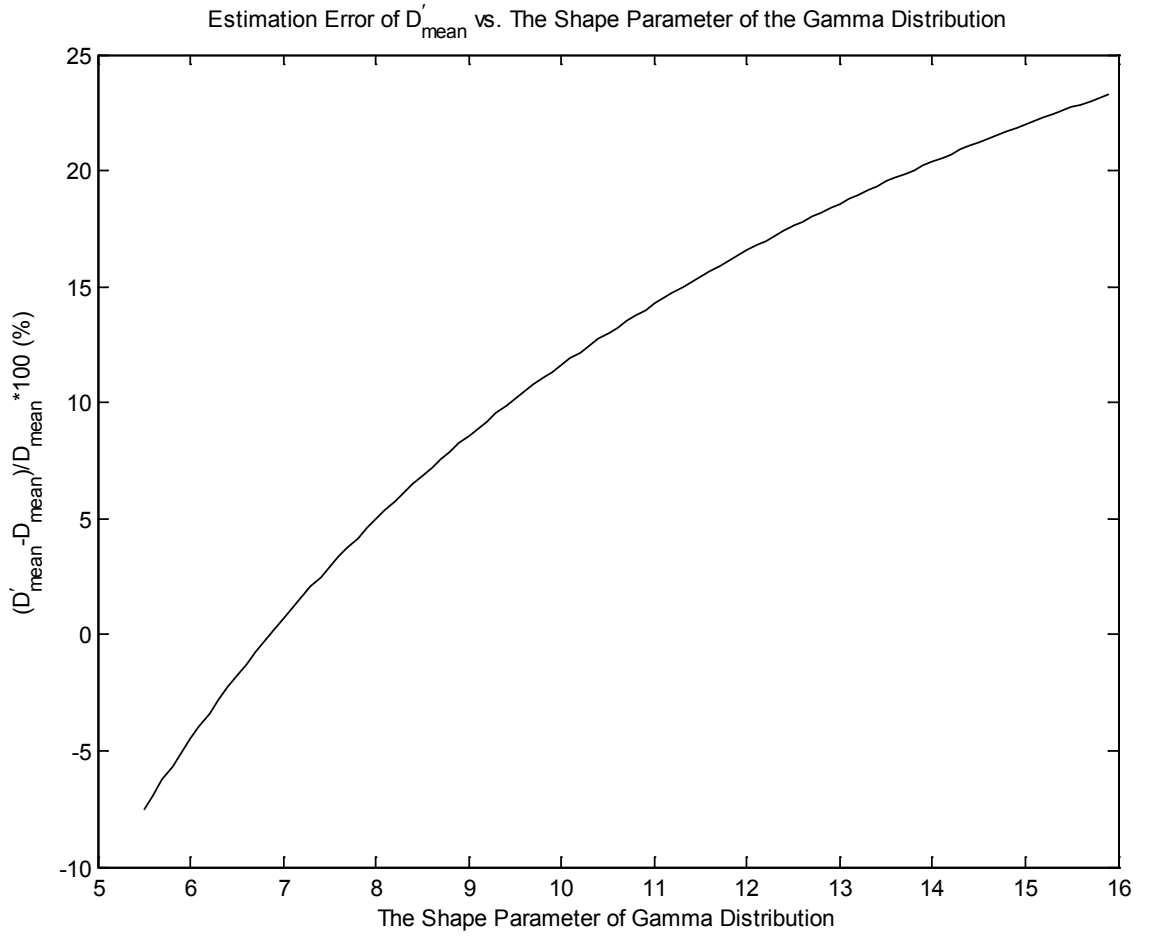

Figure 5.2: Using the lidar-radar effective diameter derived from the random sampling of the cumulative distribution function in Figure 4.1.1 and the shape parameter range of 5.5 to 15.9 given Miles et al. (2000), we show the estimation error of the lidar-radar mean diameter as a function of gamma distribution shape parameters.

Given Slingo's (1990) argument that a decrease of 15-20% in drop size is sufficient to offset a doubling of carbon dioxide concentrations, a smaller lidar-radar estimation error range is needed to describe percentage changes in drop size. To achieve a smaller error range, more in situ measurements from airborne probes and laboratory clouds would likely further constrain the gamma parameters thus leading to more accurate results. Currently the gamma parameter range compiled by Miles et al. (2000) is too large to accurately describe the laboratory drizzling cloud.
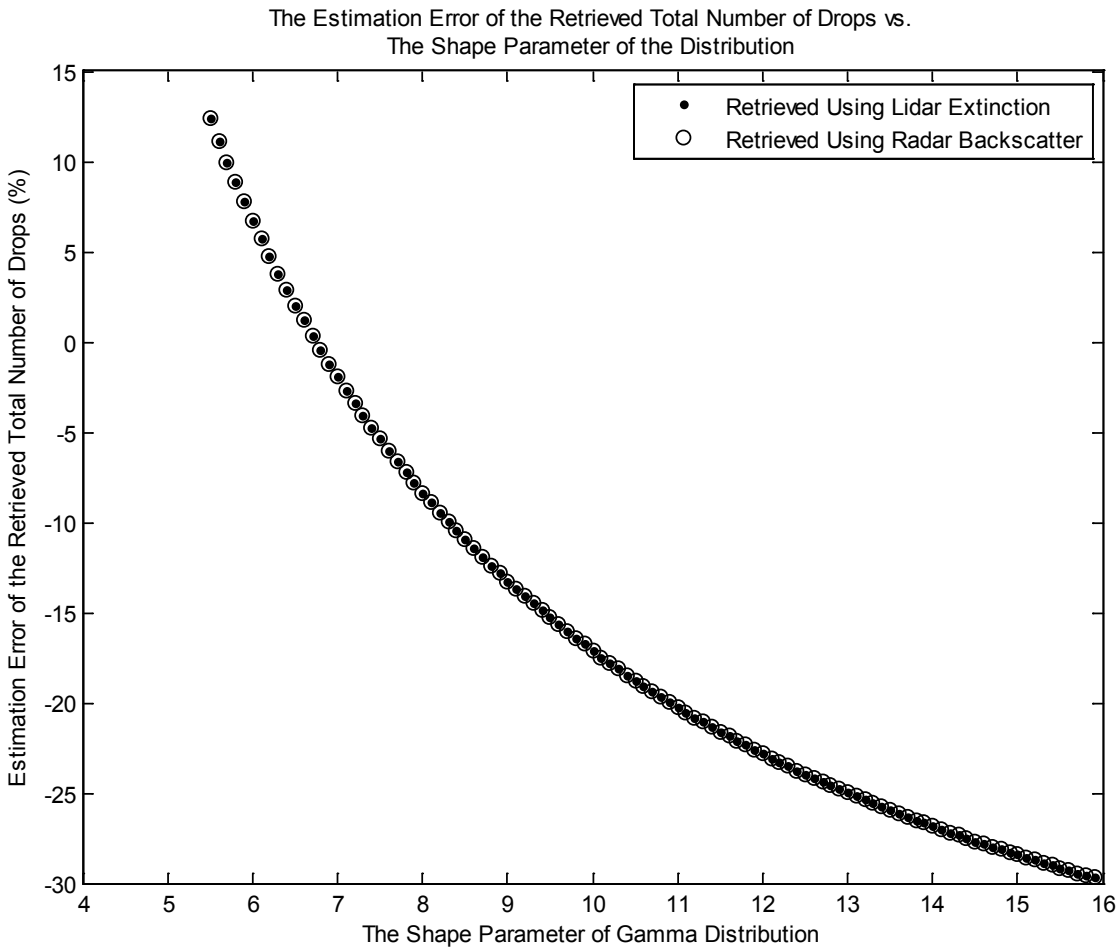

Figure 5.3: Using the lidar-radar-derived lidar-radar effective diameter from the random sampling of a distribution (parameterized from the cloud chamber PDF) and the shape parameter range of 5.5 to 15.9 from Miles et al. (2000), we show the estimation error of the total number of drops as a function of gamma distribution shape parameters. The total number of drops in a given sample volume was computed using either the second moment of the distribution and the lidar extinction cross section (dots) or the sixth moment of the distribution and the radar backscatter cross section (circles).

6 Conclusion

We simulated the results of lidar and radar scattering from a laboratory cloud to retrieve the mean diameter and the total number of gamma-distributed drop sizes in a sample volume. The lidar-radar mean diameter is retrieved within only a few percent of the true mean. In addition, the calculated total number of drops is retrieved within a few percent of the true value if only the lidar extinction cross section is used. However, if the radar backscatter cross section is used the total number of drops is not retrieved as well. In practice, the gamma distribution parameters are not known. To set bounds, a range of in situ measured gamma parameters were used to convert the lidar-radar effective diameter to a mean diameter. The estimated means varied within 13% below to 18% above the true mean. The total number of drops varied within 23% below to 27% above the true number of drops.

Due to the fact that lidars and radars sample a much larger number of drops than the number sampled from the laboratory cloud, we created a representative gamma distribution with a shape parameter $a = 7$ and a scale parameter $b = 4$ (the gamma parameters from the laboratory cloud). The distribution was randomly sampled to generate lidar extinction and radar backscatter data. Using the lidar-radar effective diameter and a range of in situ gamma parameters, the mean diameter and total number of drops in the sample volume were calculated. The total number of drops varied within 30% below to 12% above the true number of drops. The lidar-radar mean diameter varied within 8% below to 24% above the true mean.

To put the range of uncertainty for lidar-radar retrievals in perspective, a decrease of 15-20% in drop size is argued to be sufficient to offset a doubling of carbon dioxide concentrations (e.g., Slingo 1990). Thus, the inherent uncertainties associated with the lidar-radar retrieval method described here are too large to be useful. More in situ measurements from airborne probes and laboratory clouds are needed to constrain the gamma parameters to achieve more accurate results.

References

Bohren, Craig F., and Donald R. Huffman. 1983. *Absorption and Scattering of Light by Small Particles*. 1 edition. New York: Wiley-VCH.

Chang, K., Bench, J., M. Brege, W. Cantrell, K. Chandrakar, D. Ciochetto, C. Mazzoleni, L. Mazzoleni, D. Niedermeier, and R.A. Shaw. In Review. "A Laboratory Facility to Study Gas-Aerosol-Cloud Interactions in a Turbulent Environment: The Π Chamber." *Bulletin of the American Meteorological Society*.

Donovan, D. P., and A.C.A.P. van Lammeren. 2001. "Cloud Effective Particle Size and Water Content Profile Retrievals Using Combined Lidar and Radar Observations - 1. Theory and Examples." *Journal of Geophysical Research-Atmospheres* 106 (D21): 27425–48. doi:10.1029/2001JD900243.

Evans, Merran, N. A. J. Hastings, Brian Peacock, and J. Brian Peacock. 1993. *Statistical Distributions*. J. Wiley.

Fielding, M. D., J. C. Chiu, R. J. Hogan, G. Feingold, E. Eloranta, E. J. O'Connor, and M. P. Cadeddu. 2015. "Joint Retrievals of Cloud and Drizzle in Marine Boundary Layer Clouds Using Ground-Based Radar, Lidar and Zenith Radiances." *Atmos. Meas. Tech.* 8 (7): 2663–83. doi:10.5194/amt-8-2663-2015.

Hu, Y. X., and K. Stamnes. 1993. "An Accurate Parameterization of the Radiative Properties of Water Clouds Suitable for Use in Climate Models." *Journal of Climate* 6 (4): 728–42. doi:10.1175/1520-0442(1993)006<0728:AAPOTR>2.0.CO;2.

Kostinski, A. B. 2008. "Drizzle Rates versus Cloud Depths for Marine Stratocumuli." *Environmental Research Letters* 3 (4): 045019. doi:10.1088/1748-9326/3/4/045019.

Miles, Natasha L., Johannes Verlinde, and Eugene E. Clothiaux. 2000. "Cloud Droplet Size Distributions in Low-Level Stratiform Clouds." *Journal of the Atmospheric Sciences* 57 (2): 295–311. doi:10.1175/1520-0469(2000)057<0295:CDSDIL>2.0.CO;2.

O'Connor, Ewan J., Robin J. Hogan, and Anthony J. Illingworth. 2005. "Retrieving Stratocumulus Drizzle Parameters Using Doppler Radar and Lidar." *Journal of Applied Meteorology* 44 (1): 14–27. doi:10.1175/JAM-2181.1.

Petty, Grant W., and Wei Huang. 2011. "The Modified Gamma Size Distribution Applied to Inhomogeneous and Nonspherical Particles: Key Relationships and Conversions." *Journal of the Atmospheric Sciences* 68 (7): 1460–73. doi:10.1175/2011JAS3645.1.

Ramanathan, V., R. D. Cess, E. F. Harrison, P. Minnis, B. R. Barkstrom, E. Ahmad, and D. Hartmann. 1989. "Cloud-Radiative Forcing and Climate: Results from the Earth Radiation Budget Experiment." *Science* 243 (4887): 57–63. doi:10.1126/science.243.4887.57.

Ricchiazzi, Paul, Shiren Yang, Catherine Gautier, and David Sowle. 1998. "SBDART: A Research and Teaching Software Tool for Plane-Parallel Radiative Transfer in the Earth's Atmosphere." *Bulletin of the American Meteorological Society* 79 (10): 2101–14. doi:10.1175/1520-0477(1998)079<2101:SARATS>2.0.CO;2.

Siebert, H., M. Beals, J. Bethke, E. Bierwirth, T. Conrath, K. Dieckmann, F. Ditas, et al. 2013. "The Fine-Scale Structure of the Trade Wind Cumuli over Barbados – an Introduction to the CARRIBA Project." *Atmos. Chem. Phys.* 13 (19): 10061–77. doi:10.5194/acp-13-10061-2013.

Slingo, A. 1990. "Sensitivity of the Earth's Radiation Budget to Changes in Low Clouds." *Nature* 343 (6253): 49–51. doi:10.1038/343049a0.

Stephens, Graeme L. 1994. *Remote Sensing of the Lower Atmosphere: An Introduction*. New York: Oxford University Press.

Stephens, Graeme L., Si-Chee Tsay, Paul W. Stackhouse, and Piotr J. Flatau. 1990. "The Relevance of the Microphysical and Radiative Properties of Cirrus Clouds to Climate and Climatic Feedback." *Journal of the Atmospheric Sciences* 47 (14): 1742–54. doi:10.1175/1520-0469(1990)047<1742:TROTMA>2.0.CO;2.

Tas, E., A. Teller, O. Altaratz, D. Axisa, R. Bruintjes, Z. Levin, and I. Koren. 2015. "The Relative Dispersion of Cloud Droplets: Its Robustness with Respect to Key Cloud Properties." *Atmos. Chem. Phys.* 15 (4): 2009–17. doi:10.5194/acp-15-2009-2015.

Wood, Robert. 2012. "Stratocumulus Clouds." *Monthly Weather Review* 140 (8): 2373–
      2423. doi:10.1175/MWR-D-11-00121.1.

Appendix A: Comparing the number of drops in a Lidar sample volume to the number in a Radar sample volume

High Spectral Resolution Lidar
(532nm)

V=0.038 m³

# of droplets in
V ≈ 4 million
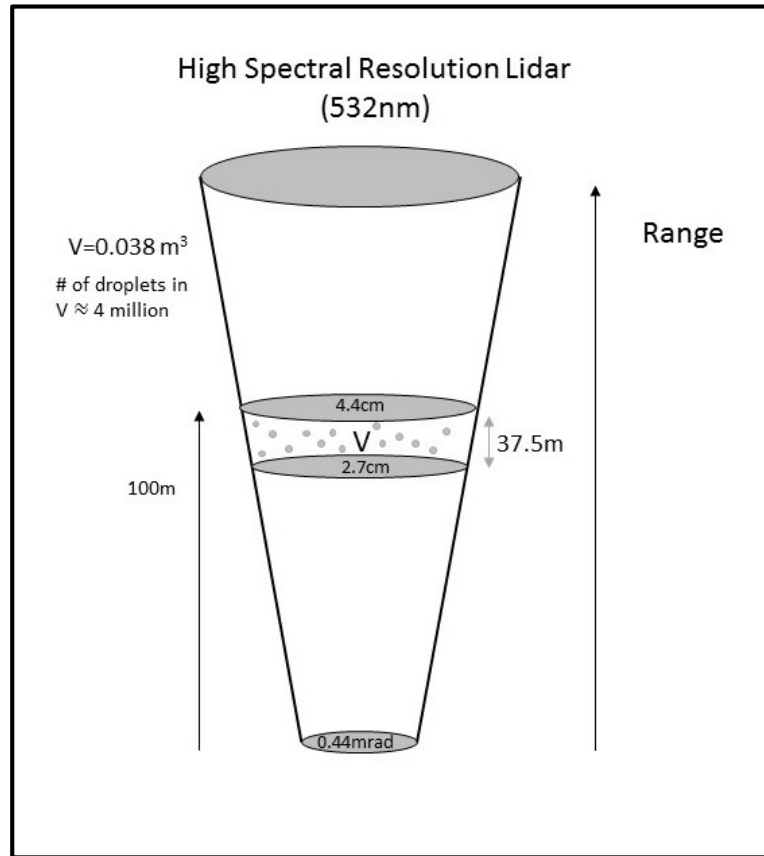
Range

4.4cm

V

37.5m

2.7cm

100m

0.44mrad

Figure A.1: Sample Volume from a High Spectral Resolution Lidar.

Given the lidar's field of view (FOV) of 0.025 degrees (CSET Website-https://www.eol.ucar.edu/field_projects/cset), we calculate the number of droplets in a lidar sample volume:

$$Footprint\ Diameter = FOV * range$$

$$Volume = \frac{\pi h}{3}\left(\frac{D^2}{4} + \frac{Dd}{4} + \frac{d^2}{4}\right)$$

where h is sample volume height (37.5m in this case), D is the footprint diameter at the far range of 100m, and d is the footprint diameter at the near range of 62.5m. Using an

estimated number density of 100 $\frac{droplets}{cm^3}$ yields a volume of approximately 4 million drops.

The radar's field of view is 0.68 degrees (CSET Website - https://www.eol.ucar.edu/field_projects/cset). The same number density yields a radar sample volume of approximately 3 billion drops, almost 3 orders of magnitude greater than the lidar sample volume.
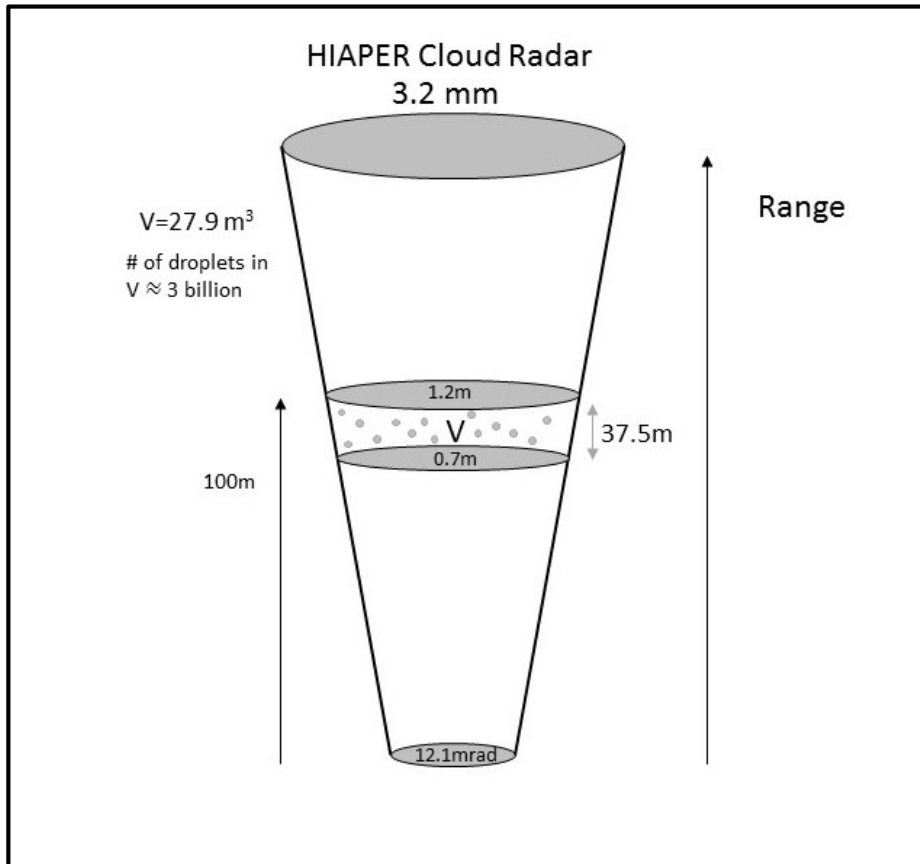

Figure A.2: Sample Volume from the HIAPER Cloud Radar.